

## NGC 1868: A METAL-POOR INTERMEDIATE-AGE CLUSTER IN THE LARGE MAGELLANIC CLOUD

PHILLIP J. FLOWER<sup>1</sup>  
 Clemson University

AND

DOUG GEISLER, PAUL HODGE,<sup>1</sup> AND EDWARD W. OLSZEWSKI  
 University of Washington

*Received 1979 June 4; accepted 1979 August 6*

### ABSTRACT

NGC 1868 is a rich, blue globular-like cluster in the LMC, located sufficiently far from the main body of the Cloud to allow accurate faint photometry of its stars. Its C-M diagram shows a well-populated main sequence with a turnoff at  $M_V \approx +0.4$ . The well-populated giant branch is much too blue to fit models with solar metals abundance. It has its faint red giants at  $B - V = +0.70$ ,  $M_V = +1.0$ , and a blue loop at  $M_V = 0.0$  extending to  $B - V = +0.50$ . The brightest red giants reach  $M_V \sim -0.5$  and  $B - V = 1.15$ . The best fit of the giant branch is with a  $Z$  of 0.001, a turnoff mass of  $2.0 M_\odot$ , and an age of  $7 \times 10^8$  years. Ten anomalously bright giants are found near the center of the cluster, and several hypotheses are suggested to explain them.

The field stars near the cluster make up a population with a few stars of the cluster age, but the majority are older stars.

*Subject headings:* clusters: globular — galaxies: Magellanic Clouds

### I. INTRODUCTION

The “blue globular” clusters of the LMC are a unique resource for the study of stellar evolution. They contain large numbers of giants and provide therefore an excellent means for comparing intermediate-mass stellar evolutionary tracks with a sample of stars of uniform distance, composition, and age. We have published previous comparisons for clusters in the age range  $5 \times 10^7$  to  $7 \times 10^7$  years (Hodge 1961*a*; Flower and Hodge 1975; Baird *et al.* 1974; Flower 1976), and others have also exploited this important resource (e.g., Gascoigne 1966; Arp and Thackeray 1967; Meyer-Hofmeister 1969; Tift and Connolly 1973; Robertson 1974; Gascoigne *et al.* 1976; Harris and Deupree 1976; Walker 1979).

Since only a small range in age has been sampled so far, we felt it appropriate to study a cluster that might be presumed to be much older. NGC 1868 was chosen for several reasons: (1) in integrated color, the cluster is redder than the others we have studied (observed  $B - V = 0.45$ ); (2) the magnitudes of the brightest stars are fainter; and (3) the cluster is in a sparsely populated region of the LMC. This cluster thus promises to be older than previously studied blue globulars in the LMC and to be in a position which minimizes the problem of crowding of images by LMC background stars.

In this paper, we present photometry of stars in NGC 1868, and compare the resulting color-magnitude

diagram with theoretical tracks constructed with a modified Paczyński code (Flower 1976). This comparison allows us to estimate the age and metal abundance of NGC 1868, providing another important clue to the history of star and cluster formation in the LMC.

### II. OBSERVATIONS

The observational data used here were obtained at the Cerro Tololo Inter-American Observatory during 1976 January and February. A series of 16 plates in  $B$  and  $V$  was obtained at the prime focus of the CTIO 4 m telescope (Table 1). All plates were calibrated for relative intensities with a sensitometer, mounted in the telescope plateholder. An auxiliary wedge (Pickering 1891; Racine 1969) of 18 cm diameter was placed in the telescope beam to form secondary images for use in extending the photometry to faint limits.

To calibrate the photographic data, a series of 20 stars was measured photoelectrically with the CTIO 1.5 m and 0.9 m telescopes (Fig. 1 and Table 2). The magnitudes of these primary standards ranged from 11.04 to 19.03 in  $B$  and from 10.09 to 17.36 in  $V$ . The photoelectric magnitudes were determined by comparison with equatorial  $UBV$  standards. For 12 of the stars, secondary images were usable (labeled in Table 2 with asterisks) and these gave values of  $B$  to 21.94 and of  $V$  to 20.95.

### III. DATA REDUCTIONS

A Cuffey iris astrophotometer was used in the reduction of all plates. Each plate was calibrated by

<sup>1</sup> Visiting Astronomer, Cerro Tololo Inter-American Observatory, operated by Associated Universities for Research in Astronomy, Inc., under contract to the National Science Foundation.

TABLE 1  
PLATES OF NGC 1868

Plate Number	Date (1976)	Exposure (minutes)	Color
1595.....	January 28	30	B
1596.....	January 28	30	B
1601.....	January 28	30	V
1602.....	January 28	30	V
1627.....	January 29	2	V
1631.....	January 29	2	B
1666.....	February 3	10	V
1667.....	February 3	60	V
1668.....	February 3	2	V
1669.....	February 3	0.5	V
1673.....	February 3	2	B
1674.....	February 3	60	B
1675.....	February 3	0.5	B
1687.....	February 4	10	B
1688.....	February 4	10	B
1694.....	February 4	10	V

fitting the standard stars to a fourth order least squares polynomial. In determining the calibration, we discarded star  $N$ , which was found to have discordant magnitudes on all plates, and usually the next most ill-fitting star. Color coefficients, which correct the photographic magnitude to the photoelectric  $UBV$  system, were also determined in the polynomial fit. The form of the correction is

$$V_{pg} = V_{pe} + K_V(B - V)_{pe},$$

$$B_{pg} = B_{pe} + K_B(B - V)_{pe}.$$

$K_V$  ranged from  $-0.04$  to  $-0.26$ , with an average of  $-0.17$ , while  $K_B$  varied from  $-0.02$  to  $-0.20$ , with an average of  $-0.10$ . Both  $K_V$  and  $K_B$  varied mostly with exposure time, with the color coefficients for equal exposure plates agreeing quite well. To calibrate the auxiliary wedge, plates of the well studied cluster NGC 2477 were taken on four of the nights. Using the values of  $V$  and  $B - V$  from Hartwick, Hesser, and McClure (1972), magnitude differences of the primary and secondary images of the brighter stars were determined. Nightly values of the difference ranged from 6.81 to 7.01 mag for the five primary standards that were bright enough to produce measurable secondary images. The best value was taken to be the average of the six plates, yielding 6.88 mag, with a standard deviation of 0.13 mag. This value agrees well with the canonical value of 6.92 mag given in the CTIO facilities manual.

The cluster (Fig. 2) was divided into three main regions: a central region which was measurable only on the shortest exposure plates (Fig. 2a); an inner annulus of radii 30"–60", and an outer region of radii 60"–90". Sixteen plates of the cluster were used, and on six of these plates the field stars (§ IV) were also measured. In addition to being irised, the inner stars that are numbered in Figure 2a had magnitudes

TABLE 2  
PHOTOELECTRIC SEQUENCE

Star	$V$	$B - V$	$N$
A.....	10.13	1.62	4
B.....	11.86	0.68	3
C.....	11.70	1.20	3
D.....	12.14	0.60	3
E.....	12.37	0.50	3
F.....	13.46	0.37	2
G.....	13.56	0.92	1
H.....	13.47	1.09	3
I.....	14.89	0.73	2
J.....	15.22	0.84	3
K.....	15.73	0.60	1
L.....	16.83	1.52	2
M.....	16.58	0.69	1
N.....	17.36	1.67	1
Q.....	16.08	0.56	1
W.....	15.25	0.76	2
X.....	14.07	0.99	2
F1.....	10.09	0.95	3
F2.....	12.09	0.74	3
F3.....	11.39	0.46	3
A*.....	17.01	...	...
B*.....	18.74	...	...
C*.....	18.58	...	...
D*.....	19.02	...	...
E*.....	19.25	...	...
F*.....	20.34	...	...
G*.....	20.44	...	...
H*.....	20.35	...	...
X*.....	20.95	...	...
F1*.....	16.97	...	...
F2*.....	18.97	...	...
F3*.....	18.27	...	...

derived via visual inspection, involving comparison of their diameters and density profiles to standard stars. These results were averaged with the iris measurements to determine final values for  $V$  and  $B - V$ .

A color-magnitude diagram of the cluster (Fig. 3) was constructed by forming eight plate pairs and averaging the colors and magnitudes determined from those pairs. Table 3 gives  $V$ ,  $B - V$ , their standard deviations, and the number of measures for all stars with  $V < 20$  mag. Stars were measured to  $V \sim 21$  mag; however, the lack of faint standards and crowding and background effects made the results for stars fainter than  $V = 20$  uncertain; hence these stars are not shown in the color-magnitude diagram. *Virtually all stars fainter than  $V = 20$  did fall clearly along a well-defined main sequence.*

Comparison of plate pairs of different exposure times indicated a significant systematic difference for  $V > 19$  mag, although pairs of equal exposure time agreed well. We concluded that background contamination was chiefly responsible and attempted to quantify and correct for this effect. Several plates were remeasured with a tighter iris and stars on several plates were scanned with a microdensitometer. Results of these attempts were inconclusive, with no improvement of the standard deviation of the magnitudes, leading us to abandon these efforts.

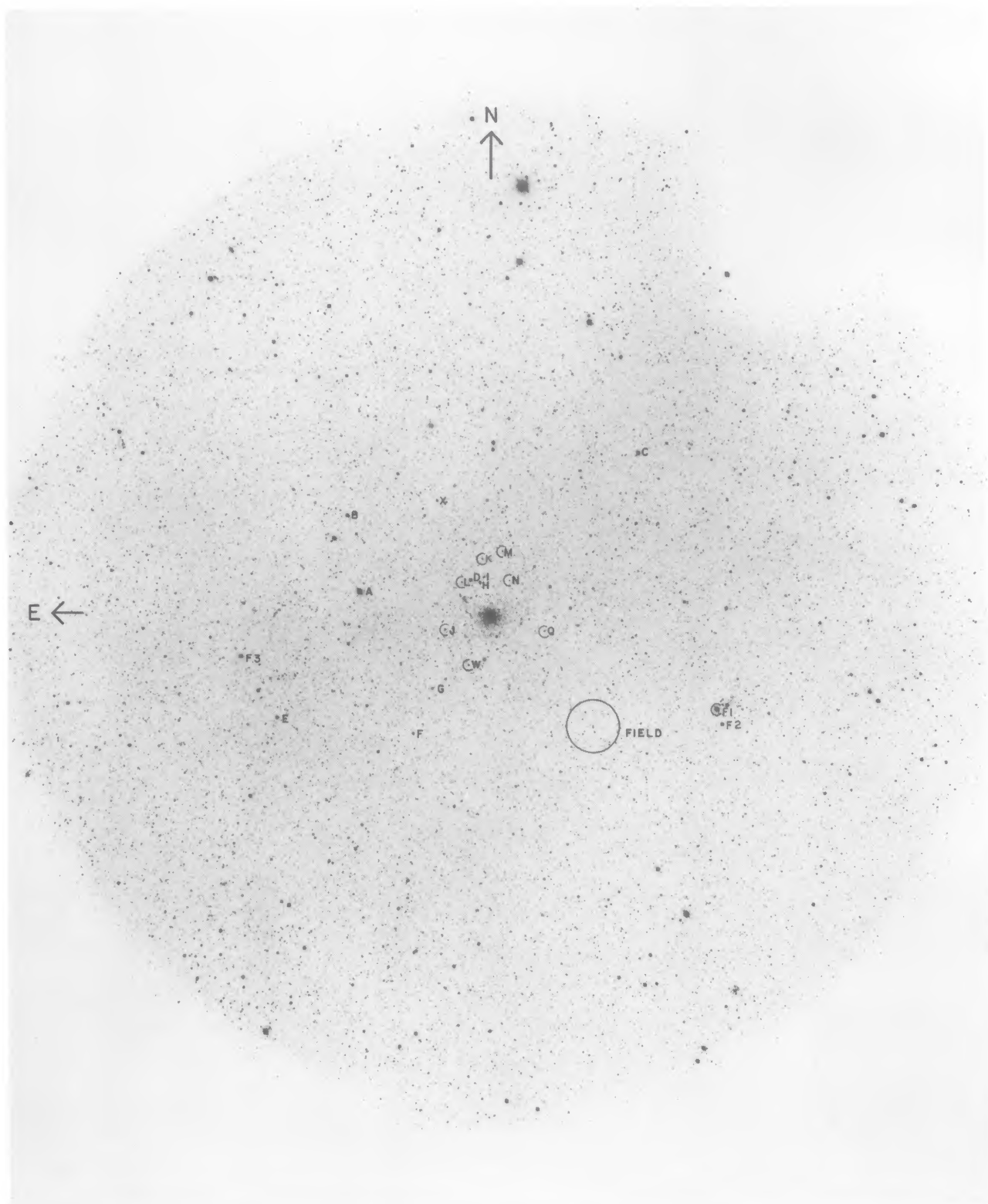


FIG. 1.—NGC 1868 and the measured adjacent field. Photoelectric standards are identified. From a 30 minute  $V$  plate.

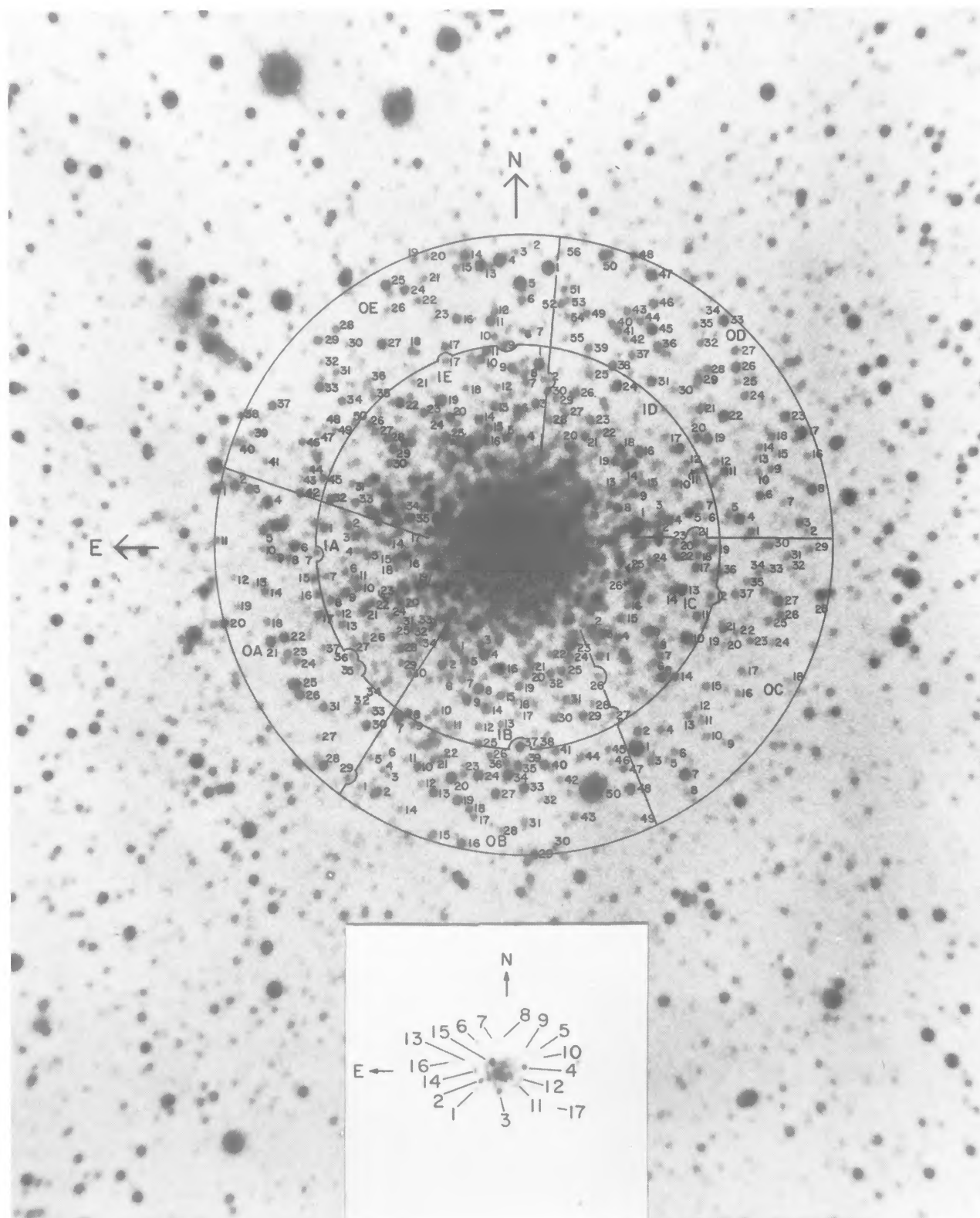


FIG. 2.—Measured stars in NGC 1868 from a 30 minute  $V$  plate. The insert shows the central stars (C prefix in Table 3) and is from a 30 second  $V$  plate.

TABLE 3  
PHOTOGRAPHIC MEASUREMENTS

Star	$V$	$\sigma(V)$	$B - V$	$\sigma(B - V)$	$N$	Star	$V$	$\sigma(V)$	$B - V$	$\sigma(B - V)$	$N$
OA 1...	18.76	0.08	0.79	0.09	5	OD 46...	19.85	0.14	0.12	0.13	5
OA 2...	19.22	0.05	1.40	0.21	5	OD 47...	18.67	0.05	0.78	0.07	5
OA 3...	19.49	0.15	0.09	0.18	5	OD 48...	19.84	0.14	0.05	0.18	5
OA 4...	18.71	0.12	0.66	0.07	5	OD 49...	19.98	0.15	0.11	0.23	5
OA 5...	19.39	0.17	0.01	0.13	5	OD 50...	18.89	0.14	0.69	0.15	3
OA 6...	18.82	0.12	0.11	0.15	5	OD 52...	19.90	0.11	0.04	0.09	5
OA 15...	19.92	0.12	0.19	0.16	5	OE 1...	17.76	0.14	1.16	0.13	6
OA 16...	19.97	0.14	0.13	0.14	5	OE 4...	17.93	0.16	1.12	0.14	6
OA 17...	19.56	0.17	0.03	0.16	5	OE 5...	17.97	0.13	1.07	0.13	6
OA 20...	19.28	0.12	0.51	0.15	5	OE 6...	19.91	0.15	0.07	0.12	5
OA 21...	19.00	0.09	0.71	0.04	5	OE 9...	19.95	0.20	0.03	0.19	5
OA 22...	19.24	0.10	0.73	0.15	5	OE 11...	19.14	0.13	0.78	0.17	5
OA 23...	19.74	0.13	0.03	0.14	5	OE 13...	18.37	0.07	1.03	0.09	6
OA 25...	18.43	0.16	0.61	0.12	4	OE 14...	19.68	0.21	1.05	0.30	5
OA 26...	18.98	0.09	0.79	0.11	5	OE 16...	19.71	0.08	1.22	0.22	5
OA 28...	19.29	0.15	0.03	0.17	5	OE 17...	19.83	0.15	0.12	0.16	5
OA 30...	19.45	0.10	0.53	0.15	5	OE 18...	19.99	0.17	0.37	0.13	5
OA 31...	19.82	0.13	0.07	0.14	5	OE 14...	19.47	0.11	0.06	0.13	5
OB 2...	19.21	0.23	-0.05	0.15	5	OE 25...	19.01	0.10	0.75	0.13	5
OB 7...	18.93	0.19	0.71	0.12	5	OE 27...	19.15	0.09	0.75	0.15	5
OB 8...	19.44	0.17	0.60	0.19	5	OE 33...	19.15	0.19	-0.18	0.16	5
OB 10...	19.67	0.11	0.75	0.12	5	OE 34...	19.84	0.13	0.15	0.18	5
OB 13...	19.55	0.13	0.22	0.15	5	OE 37...	19.68	0.11	0.34	0.10	5
OB 16...	19.59	0.10	0.72	0.16	5	OE 42...	19.71	0.15	0.03	0.18	5
OB 18...	20.00	0.14	0.12	0.12	5	OE 45...	19.74	0.12	0.03	0.15	5
OB 19...	19.24	0.12	0.09	0.14	5	IA 1...	19.63	0.17	0.03	0.15	5
OB 20...	18.64	0.05	1.00	0.11	5	IA 2...	19.76	0.16	0.02	0.17	5
OB 24...	18.99	0.05	0.79	0.07	5	IA 3...	19.42	0.27	0.00	0.16	5
OB 25...	19.85	0.14	0.12	0.20	5	IA 8...	19.88	0.13	0.05	0.18	5
OB 27...	19.50	0.11	0.67	0.23	5	IA 9...	19.44	0.11	0.57	0.10	5
OB 29...	19.30	0.12	0.75	0.14	5	IA 10...	19.68	0.24	-0.02	0.17	5
OB 33...	18.92	0.07	0.75	0.13	5	IA 11...	19.90	0.23	0.06	0.13	5
OB 34...	18.54	0.13	0.56	0.13	5	IA 14...	19.84	0.21	0.00	0.16	5
OB 35...	19.53	0.26	-0.04	0.21	5	IA 15...	19.18	0.36	-0.01	0.22	5
OB 37...	19.06	0.06	0.70	0.10	5	IA 16...	18.86	0.40	-0.51	0.18	4
OB 40...	19.42	0.17	0.67	0.22	5	IA 17...	19.22	0.39	-0.08	0.21	5
OB 41...	19.86	0.13	0.09	0.18	5	IA 19...	18.17	0.18	0.91	0.11	5
OB 47...	19.98	0.13	0.10	0.18	5	IA 20...	19.09	0.13	0.52	0.14	5
OB 48...	18.94	0.06	0.73	0.08	5	IA 21...	19.25	0.32	-0.10	0.18	4
OB 50...	14.52	0.04	0.73	0.06	7	IA 22...	19.64	0.30	0.06	0.20	5
OC 1...	16.89	0.06	1.44	0.07	7	IA 28...	19.66	0.13	0.13	0.14	5
OC 2...	19.42	0.18	0.18	0.18	5	IA 32...	19.75	0.19	0.02	0.10	5
OC 7...	18.45	0.05	0.96	0.09	6	IA 33...	19.63	0.26	0.02	0.18	5
OC 13...	19.93	0.11	0.23	0.18	5	IB 1...	19.35	0.27	0.90	0.17	5
OC 14...	19.59	0.14	-0.05	0.17	5	IB 2...	19.32	0.13	0.68	0.14	5
OC 21...	19.71	0.16	0.52	0.11	5	IB 3...	19.42	0.21	0.70	0.21	5
OC 26...	19.81	0.13	0.06	0.13	5	IB 4...	18.07	0.06	1.08	0.07	5
OC 27...	18.68	0.13	0.54	0.09	5	IB 5...	19.03	0.16	0.03	0.14	5
OC 28...	18.39	0.02	1.12	0.06	5	IB 8...	18.49	0.08	0.13	0.09	5
OC 36...	19.78	0.23	0.03	0.15	5	IB 9...	19.14	0.12	0.72	0.11	5
OD 1...	19.91	0.15	0.03	0.17	5	IB 14...	19.67	0.24	0.04	0.23	5
OD 3...	19.82	0.13	0.69	0.16	5	IB 15...	19.80	0.17	0.01	0.14	5
OD 4...	18.55	0.09	0.40	0.08	5	IB 16...	18.02	0.25	0.55	0.11	6
OD 5...	19.98	0.16	0.16	0.13	5	IB 19...	19.66	0.15	0.02	0.16	5
OD 6...	19.64	0.07	0.67	0.14	5	IB 20...	19.82	0.29	0.17	0.15	5
OD 8...	18.94	0.06	0.71	0.09	5	IB 21...	19.38	0.22	0.07	0.14	5
OD 11...	19.49	0.17	0.37	0.17	5	IB 23...	17.95	0.24	0.92	0.08	6
OD 17...	17.88	0.21	-0.04	0.15	6	IB 24...	19.70	0.27	0.34	0.13	5
OD 19...	19.42	0.21	0.00	0.22	5	IB 25...	19.63	0.15	0.65	0.22	5
OD 20...	19.60	0.15	0.62	0.15	5	IB 29...	19.59	0.16	0.15	0.14	5
OD 21...	19.64	0.18	0.05	0.13	5	IB 30...	19.83	0.15	0.14	0.11	5
OD 22...	18.81	0.05	0.97	0.12	5	IB 31...	19.95	0.16	0.09	0.17	5
OD 23...	19.10	0.06	0.81	0.08	5	IB 32...	19.61	0.20	0.25	0.27	4
OD 24...	19.94	0.11	0.02	0.15	5	IC 1...	19.34	0.19	0.07	0.10	5
OD 26...	19.24	0.14	0.01	0.17	5	IC 2...	19.10	0.32	0.41	0.15	4
OD 29...	19.81	0.20	-0.06	0.29	5	IC 3...	18.63	0.20	0.87	0.10	5
OD 31...	19.31	0.10	0.72	0.21	5	IC 4...	19.59	0.19	0.17	0.18	5
OD 33...	18.86	0.04	0.79	0.08	5	IC 5...	18.80	0.17	-0.11	0.18	5
OD 36...	19.54	0.20	-0.01	0.16	5	IC 7...	19.75	0.18	0.06	0.21	5
OD 38...	19.60	0.10	0.68	0.14	5	IC 8...	19.81	0.19	0.06	0.20	5
OD 41...	19.79	0.17	0.15	0.13	5	IC 9...	18.59	0.12	0.62	0.07	5
OD 44...	19.98	0.14	0.08	0.15	5	IC 10...	18.25	0.11	0.84	0.07	6
OD 45...	18.95	0.16	0.68	0.13	5	IC 11...	19.52	0.16	0.12	0.19	5

TABLE 3—Continued

Star	$V$	$\sigma(V)$	$B - V$	$\sigma(B - V)$	$N$	Star	$V$	$\sigma(V)$	$B - V$	$\sigma(B - V)$	$N$
IC 13...	18.53	0.19	0.56	0.13	5	IE 9...	19.42	0.20	0.03	0.19	5
IC 14...	19.29	0.32	0.71	0.18	5	IE 10...	19.49	0.14	0.64	0.12	5
IC 15...	19.75	0.15	0.05	0.12	5	IE 11...	19.57	0.18	0.06	0.17	5
IC 17...	19.72	0.16	0.04	0.16	5	IE 13...	19.33	0.20	0.00	0.26	5
IC 18...	19.82	0.16	0.13	0.16	5	IE 14...	19.30	0.17	-0.12	0.16	5
IC 19...	19.72	0.18	0.64	0.19	5	IE 15...	19.24	0.18	0.66	0.22	5
IC 20...	19.70	0.19	0.11	0.17	5	IE 16...	18.33	0.29	0.71	0.07	5
IC 22...	19.84	0.23	0.09	0.20	5	IE 19...	18.39	0.04	0.93	0.07	6
IC 23...	19.86	0.12	0.05	0.12	5	IE 20...	19.18	0.13	0.71	0.14	5
IC 24...	19.93	0.09	0.20	0.08	3	IE 22...	19.21	0.15	0.78	0.12	5
IC 25...	19.75	0.17	0.19	0.07	5	IE 23...	19.56	0.15	0.14	0.14	5
IC 26...	19.00	0.19	-0.01	0.21	2	IE 25...	19.10	0.49	-0.18	0.43	5
ID 1...	16.28	0.31	0.96	0.09	7	IE 26...	19.97	0.15	0.11	0.11	5
ID 2...	19.44	0.26	0.67	0.24	5	IE 27...	19.91	0.15	0.12	0.14	5
ID 3...	19.58	0.35	0.07	0.14	5	IE 28...	19.49	0.15	0.66	0.11	5
ID 4...	19.03	0.20	0.07	0.13	5	IE 29...	19.51	0.19	0.65	0.15	5
ID 5...	19.08	0.12	0.70	0.14	5	IE 30...	19.97	0.12	0.12	0.11	5
ID 7...	19.66	0.20	0.07	0.22	5	IE 32...	19.39	0.15	0.12	0.19	5
ID 8...	18.85	0.19	0.59	0.13	5	IE 33...	19.75	0.13	-0.01	0.22	5
ID 9...	19.43	0.25	0.00	0.14	5	IE 34...	19.52	0.32	-0.01	0.18	5
ID 10...	19.94	0.09	0.77	0.07	5	IE 35...	18.53	0.20	0.52	0.08	5
ID 13...	19.23	0.29	0.10	0.16	5	C 1...	16.86	0.20	0.69	0.09	4
ID 14...	19.57	0.25	0.09	0.17	5	C 2...	16.13	0.21	0.74	0.23	4
ID 15...	19.93	0.16	0.16	0.14	5	C 3...	16.01	0.38	0.09	0.26	4
ID 16...	18.94	0.20	0.10	0.18	5	C 4...	15.98	0.12	0.95	0.11	4
ID 18...	18.85	0.19	0.75	0.15	5	C 5...	16.83	0.12	0.82	0.04	3
ID 19...	19.40	0.22	0.05	0.19	5	C 6...	16.64	0.01	0.88	0.05	3
ID 20...	18.33	0.25	0.68	0.10	5	C 7...	16.92	0.12	0.75	0.14	3
ID 21...	19.39	0.18	0.07	0.16	5	C 8...	16.93	0.10	0.92	0.20	3
ID 23...	19.75	0.21	0.05	0.15	5	C 9...	17.04	0.28	0.80	0.13	3
ID 24...	18.92	0.10	0.68	0.10	5	C 10...	17.14	0.32	1.24	0.16	2
ID 29...	19.36	0.20	-0.01	0.16	5	C 11...	16.77	0.41	0.07	0.06	3
ID 30...	19.80	0.12	0.05	0.20	5	C 12...	16.70	0.20	0.45	0.15	4
IE 1...	18.59	0.05	0.98	0.06	5	C 13...	17.03	0.29	0.79	0.14	3
IE 3...	19.44	0.15	0.69	0.18	5	C 14...	16.73	0.25	0.51	0.23	3
IE 4...	18.48	0.32	-0.06	0.13	5	C 15...	15.66	0.09	0.62	0.31	3
IE 5...	19.41	0.27	0.01	0.24	5	C 16...	16.07	0.28	0.95	0.18	2
IE 6...	19.17	0.32	0.13	0.21	5	C 17...	17.53	0.55	1.24	0.52	2
IE 8...	19.97	0.19	0.16	0.14	5						

## IV. FIELD STARS

Figure 4 shows the C-M diagram of field stars sampled in an area equal to that from which the NGC 1868 stars were taken, and located approximately 7' SW of NGC 1868 (Figs. 1 and 5). The field C-M diagram is the result of averaging the colors and magnitudes derived from a 60, 30, and 10 minute plate pair. The final values are given in Table 4. A comparison with the NGC 1868 C-M diagram shows that the majority of the field stars contaminating the cluster diagram are at intermediate colors. For the stars with  $0.4 < B - V < 1.2$  and  $18 < V < 20$ , there are 81 stars in the cluster diagram and 30 in the field. Furthermore, though photometry fainter than  $V = 20$  is uncertain (see § III), we can compare numbers of stars on the main sequence. In the area bounded by  $-0.4 < B - V < 0.4$  for  $19 < V < 20$  and  $-0.4 < B - V < 0.7$  for  $V > 20$  there are 280 stars in the cluster C-M diagram and 95 in the field, which is somewhat more complete than the cluster because of lack of crowding.

Figure 6 shows a comparison of the cumulative luminosity functions of the main sequences for the cluster and field. The two differ in curvature, and this

is most likely due to a different age distribution—namely, a nearly unique age of  $\sim 7 \times 10^8$  years for NGC 1868 (see § VI) as opposed to a spread in age for the field.

The only other published field C-M diagrams for this part of the LMC are one near NGC 1831 (Hodge 1963) and one south of NGC 1866 (Field II in Hodge 1961*b*). Neither reaches such faint stars as in the present case, the first going to  $V = 19$  and the second only to  $V = 18$ . In both cases, the similarity in the distribution of the stars is clear; most are of intermediate color, with an approximately uniform distribution of stars across the diagram from  $B - V = 0$  to  $+1.2$  for magnitudes between  $V = 19$  and 16. Most of these stars are probably Galactic foreground stars (Woolley 1960). There are only about three stars in the field C-M diagram that could be classical Population II giants, suggesting that the density of very old metal-poor stars at this location in the LMC is fairly low. The number in a previous study of a field (Area I, Hodge 1961*b*) closer to the main body of the Cloud, but still in an open, sparsely populated region (for  $16 < V < 17$  and  $0.8 < B - V < 1.6$ ), is 152 stars in  $650 \text{ arcmin}^2$ . The present field is  $4.7 \text{ arcmin}^2$  in area,

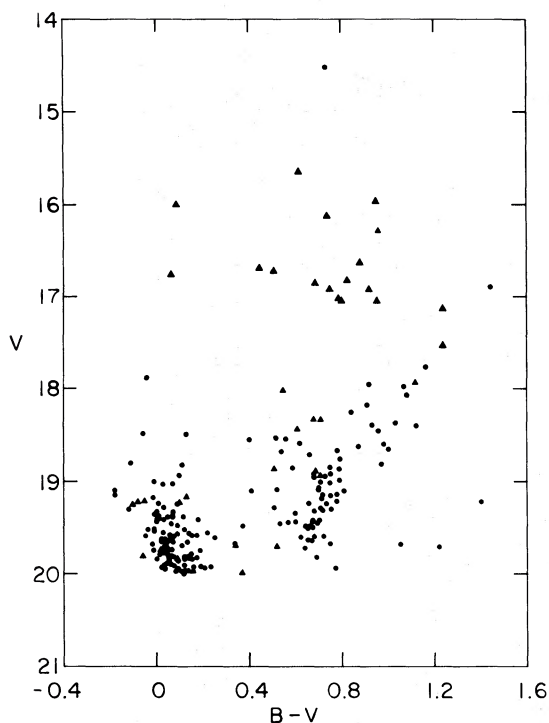


FIG. 3.—C-M diagram for NGC 1868. Triangles mark stars that were crowded.

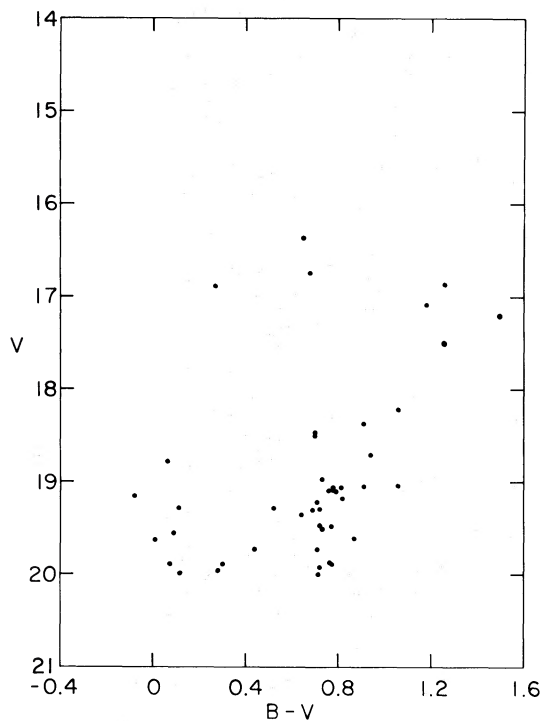


FIG. 4.—C-M diagram for stars in the comparison field.

TABLE 4  
FIELD STARS

Star	$V$	$\sigma(V)$	$B - V$	$\sigma(B - V)$	$N$
1.....	19.46	0.11	0.72	0.06	3
2.....	16.36	0.09	0.65	0.14	3
3.....	17.20	0.13	1.50	0.16	3
4.....	19.08	0.10	0.78	0.13	3
5.....	19.30	0.07	0.69	0.20	3
6.....	17.08	0.11	1.18	0.13	3
7.....	19.29	0.06	0.52	0.15	3
8.....	18.50	0.10	0.70	0.12	3
9.....	19.73	0.09	0.44	0.17	3
10.....	18.36	0.04	0.91	0.09	2
11.....	19.29	0.09	0.72	0.24	3
12.....	18.79	0.06	0.06	0.16	3
13.....	19.87	0.06	0.76	0.20	3
14.....	17.49	0.13	1.26	0.14	3
15.....	19.73	0.09	0.71	0.19	3
16.....	18.97	0.06	0.73	0.11	2
17.....	19.98	0.06	0.72	0.11	3
18.....	19.60	0.07	0.87	0.06	3
19.....	19.10	0.06	0.79	0.17	3
20.....	16.89	0.10	0.27	0.13	3
21.....	19.18	0.08	0.82	0.14	3
22.....	19.88	0.08	0.77	0.31	3
23.....	19.92	0.06	0.72	0.28	3
24.....	19.28	0.15	0.11	0.16	3
25.....	18.70	0.10	0.94	0.16	3
26.....	19.95	0.06	0.28	0.12	3
27.....	19.89	0.07	0.07	0.17	3
28.....	19.99	0.09	0.12	0.22	3
29.....	19.22	0.09	0.71	0.21	3
30.....	19.04	0.10	0.91	0.21	3
31.....	16.74	0.07	0.68	0.10	3
32.....	19.50	0.11	0.73	0.30	3
33.....	19.06	0.04	0.78	0.13	3
34.....	16.86	0.14	1.26	0.13	3
35.....	19.09	0.08	0.76	0.19	3
36.....	19.06	0.08	0.81	0.15	3
37.....	19.48	0.08	0.77	0.25	3
38.....	19.63	0.13	0.01	0.18	3
39.....	18.46	0.11	0.70	0.10	3
40.....	18.21	0.13	1.06	0.12	3
41.....	19.36	0.12	0.64	0.15	3
42.....	19.55	0.11	0.09	0.16	3
43.....	19.16	0.10	-0.08	0.12	3
44.....	19.09	0.07	0.76	0.15	3
45.....	19.88	0.08	0.30	0.20	3
46.....	19.03	0.10	1.06	0.12	2

so it has a density of such stars that is nearly the same as at the location of Area I.

#### V. THE COLOR-MAGNITUDE DIAGRAM

To compare the color-magnitude diagram of NGC 1868 with our theoretical tracks, it is necessary to remove field stars (§ IV) from the diagram. We have carried out two versions of a "correction" to Figure 3, both statistical in nature but instructive. First, we have divided the C-M diagram into rectangular components. Figure 7 shows the result of subtracting the field (control) stars in each rectangle from the NGC 1868 area stars. The result gives the approximate distribution of cluster members in the C-M diagram.

Figure 8 shows an alternative representation, easier to interpret but somewhat less justifiable statistically. To produce this figure, we have taken each point on

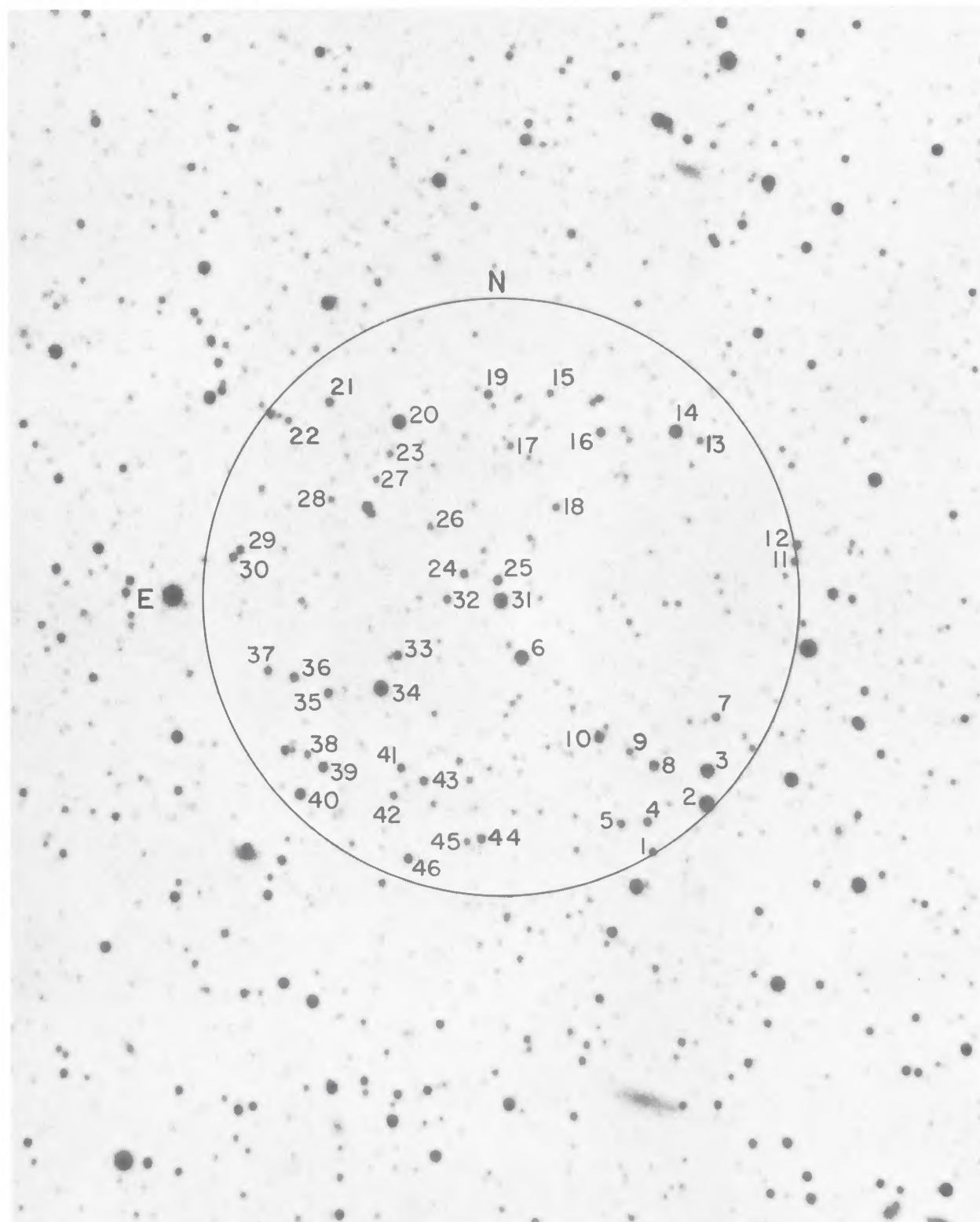


FIG. 5.—The comparison field (from a 30 minute *V* plate)

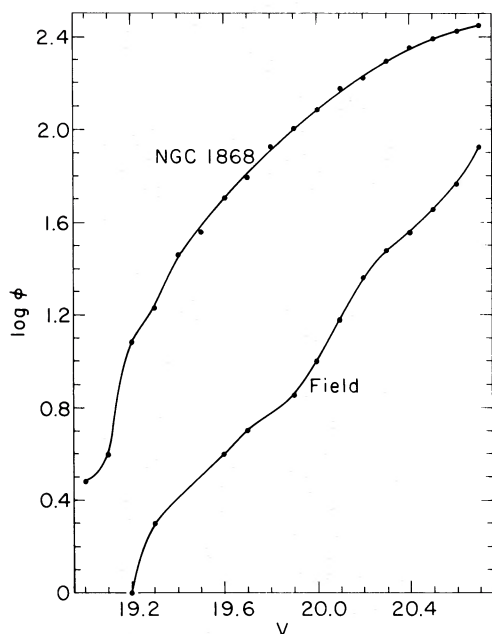


FIG. 6.—The cumulative main sequence luminosity functions for NGC 1868 and the comparison field.

the control diagram and used its position to identify the star in the NGC 1868 diagram nearest its position, which was then removed (“zapped”) from the diagram. We also eliminated those stars which were considered excessively crowded (Fig. 3, *triangles*). The zapped C-M diagram will be used in the following discussions and comparisons.

The principal features of NGC 1868’s C-M diagram are a well-populated main sequence, a broad, thinning turnoff, a Hertzsprung gap  $\sim 0.5$  mag wide in  $B - V$ , and a well-developed and complex giant branch. The overall appearance of the C-M diagram is similar to those of NGC 2209 (Gascoigne *et al.* 1976) and SL 868 (Freeman and Gascoigne 1977; Walker 1979), although the giants are bluer in NGC 1868. Our derived age for NGC 1868 is similar to the ages of NGC 2209 and SL 868; we attribute the blueness of its giants to a lower  $[\text{Fe}/\text{H}]$ , as explained in § VI.

NGC 1868 also contains approximately 10 superluminous stars in and near the center of the cluster. Because these stars are crowded (see Fig. 2), the average uncertainty in their magnitudes is 0.24 mag (see § III and Table 3). However, in view of the fact that these stars are at least 1 mag above the brightest giants, it is clear that these are indeed superluminous stars of the type discussed by Flower and Hodge (1975) for other LMC clusters.

The existence of superluminous stars in NGC 1868 is intriguing, for although such stars occur in several

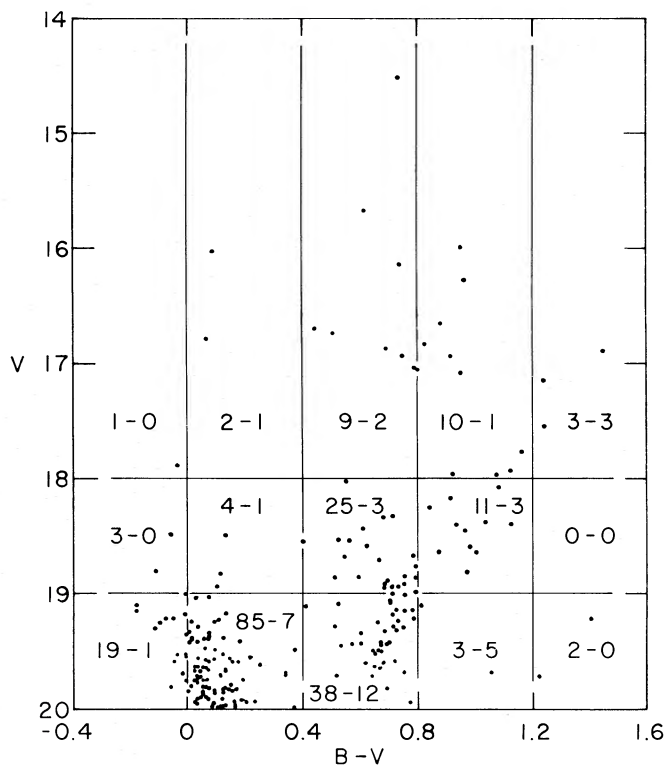


FIG. 7.—A field-cluster comparison diagram. The first number in each box is the number of stars in the NGC 1868 C-M diagram, and the second number is for the field.

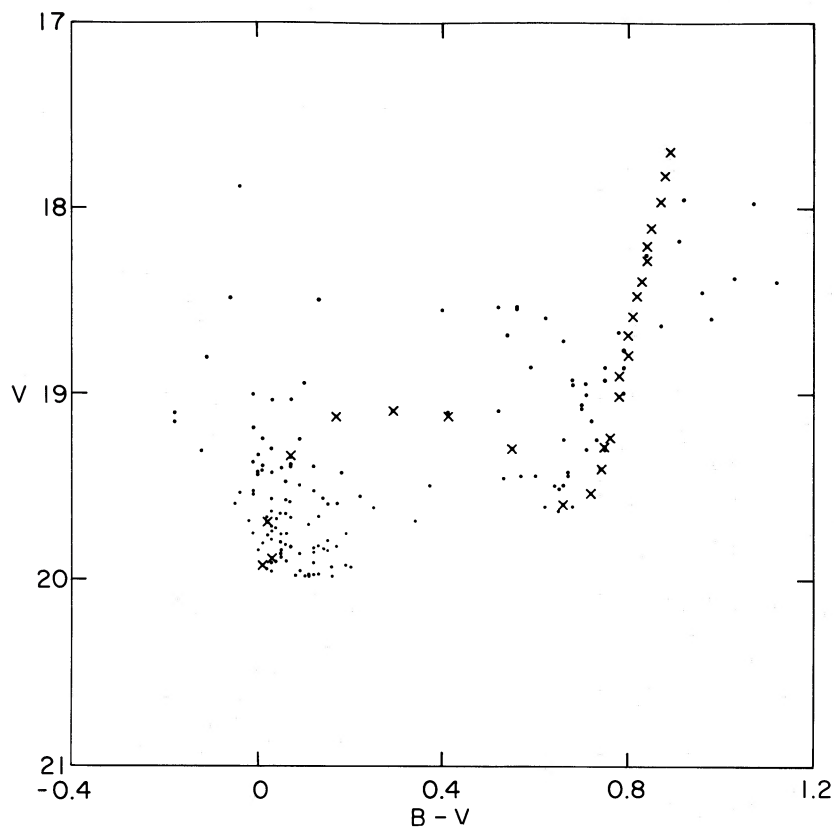


FIG. 8.—The field-corrected (“zapped”) C-M diagram for NGC 1868. Model 3 is shown for comparison. The model point at  $B - V = 0.17$ ,  $V = 19.12$ , has an age of  $6.50 \times 10^8$  years, and all subsequent points are separated by  $2 \times 10^6$  years.

LMC populous clusters, none exist in Galactic open clusters. The average properties of these stars in NGC 1868 are  $V \sim 16.7$ ,  $B - V \sim 0.8$ . There are two blue stars in this group, populating the blue side of the instability strip.

There are several possible explanations for the properties of these stars: they might be field stars, binaries, younger stars than most cluster stars, or stars in late stages of evolution. We believe that these stars are not field stars, for after the statistical subtraction of the field (see § IV) 10 stars still remain, and all of these stars are found within 5 pc of the center of the cluster. Furthermore, Flower and Hodge (1975) note the presence of similar stars in the central areas of four younger clusters. We also believe it unlikely that these stars are binaries. Cassegrain 4 m plates of NGC 2156, 2159, 2164, and 2172 taken by Flower do not resolve them. They lie more than 1 mag above the brightest giants in NGC 1868, which means that if they were multiple stars, we would have 10 examples of such stars containing what would already be the brightest cluster members, a very dubious possibility.

The possibility that they are younger stars, representing a recent burst of star formation, is also unlikely. A  $2 M_{\odot}$  model fits the main sequence and giant branch of the cluster reasonably well (§ VI). We would

expect to see many brighter main-sequence stars if there had been a recent wave of star formation in the cluster. Finally, we note the possibility that the stars are in a stage of stellar evolution beyond the second ascent of the giant branch. Such a late stage of stellar evolution is not predicted by models (§ VI); and if it exists, we presume that time scales are very short. Only in very populous clusters such as the LMC blue globulars would the possibility of seeing a short-lived phase be significant; NGC 1868 is far more massive than any known open clusters in the Galaxy. One suggestion might be that these stars are in a carbon-burning loop phase. Models, however, predict that carbon burning for stars of this mass would disrupt such stars. The superluminous stars in NGC 1868 are less bright than those in the much younger clusters NGC 2156, 2159, 2164, and 2172—a fact which suggests that, whatever their cause, their properties are related to the age of the cluster.

We will omit these stars in further diagrams since their colors and magnitudes are more uncertain than those of the bulk of the stars measured.

#### VI. COMPARISON WITH THEORY

In the following discussion we will use the distance modulus for the LMC that we obtained many years

TABLE 5

Model	Mass ( $M_{\odot}$ )	$X$	$Y$	$Z$	$I/H$	Age ( $10^8$ yr)
1.....	2.5	0.745	0.25	0.005	1.36	5.67
2.....	2.25	0.748	0.25	0.002	1.5	6.85
3.....	2.0	0.749	0.25	0.001	1.5	7.00

ago from Cepheids, 18.6 apparent (Hodge and Wright 1969). This value lies in about the middle of recently determined values, though recent criticisms (see de Vaucouleurs 1978) have pointed out that the uncertainty in these values may be larger than traditionally believed.

To determine the age and metal abundance of the cluster, we have compared the zapped color-magnitude diagram of NGC 1868 both to Yale isochrones (Ciardullo and Demarque 1977) and to tracks which we calculated with a modified Paczyński code. The best-fit Yale isochrone gives an age of  $2 \times 10^8$  years, with a turnoff mass of  $2.4 M_{\odot}$ . The usual value of the reddening for the LMC of 0.1 was adopted, which leads to a good fit of the main sequence to the Yale isochrone.

To obtain a better indication of the turnoff mass and metallicity of the cluster, three new evolutionary models were computed. The parameters for the mass, metallicity, and mixing length, and the resultant age for each model are given in Table 5, and the details of the models are given in the Appendix. The code computes the evolution of a star from the main sequence, up the giant branch to the tip, through the blue loop, and back up the giant branch. Model 3, the  $2.0 M_{\odot}$  model, was followed only part way up the first ascent of the giant branch before degeneracy set in. We note here that Alcock and Paczyński (1978) have calculated the evolution of a star with the same mass and  $Z$ , but with a mixing length of 1.0 pressure scale height, giving similar results.

To convert from the theoretical H-R diagram to the observational diagram (or vice versa) we used the  $T_{\text{eff}}:B - V$ :bolometric correction relationships from Flower (1976) and from Bell and Gustafson (1978) for the main sequence and the giants, respectively. The Bell and Gustafson theoretical relationships were used because they are the most recent and because they, unlike earlier relationships, give an excellent fit to our color-magnitude diagram.

Figure 9 shows the cluster giants together with models 2 and 3 in the theoretical plane. From the existence of stars in Figure 9 with  $\log L/L_{\odot} \sim 2.0$  and  $\log T_{\text{eff}} \sim 3.75$  and from model calculations of intermediate-mass stars (Alcock and Paczyński 1978; Becker, Iben, and Tuggle 1977; Flower 1976), one can conclude that these stars are core helium burners of low metallicity evolving through a loop phase. It is known that the existence of an extended loop in the H-R diagram performed by a model is very sensitive to stellar mass at masses below  $\sim 3 M_{\odot}$  (see, for example, the discussion by Iben and Tuggle 1975). At some mass,  $M_L$ , below  $\sim 3 M_{\odot}$ , there exists a small mass increment,  $\sim 0.3$ – $0.5 M_{\odot}$ , in which the loop

phenomenon rapidly disappears; stars more massive than  $M_L$  exhibit loops while less massive stars do not. Furthermore, as metallicity decreases,  $M_L$  decreases.

It would appear that models 2 and 3 lie close to the mass increment corresponding to their respective metallicities. Hence, a further reduction of  $Z$  could possibly lead to low-mass models that would have blue loops in the C-M diagram, representing the period during which they consume helium in their cores.

Figures 8 and 10 show model 3 superposed on the cluster color-magnitude diagram, which is shown with 1 standard deviation error bars on the giants to indicate the accuracy of the fit (Fig. 10) and without error bars (Fig. 8) to facilitate the comparison. In general, the observations and theory compare well. There are, however, two interesting differences: (1) there appears

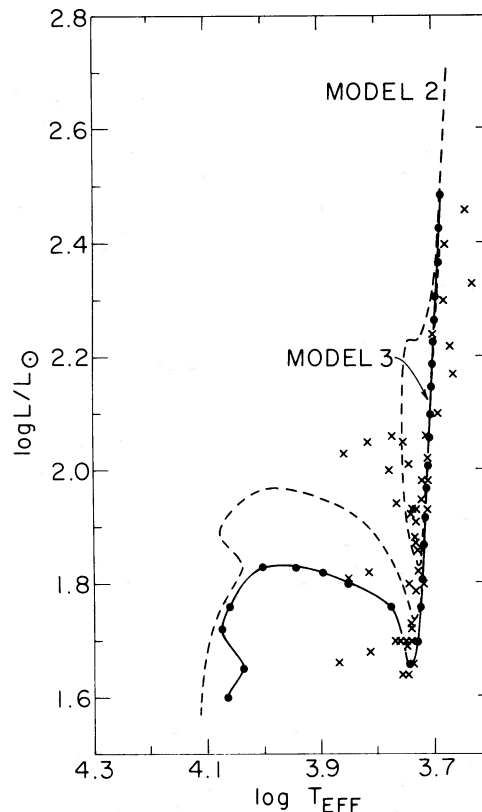


FIG. 9.—Theoretical T-L diagram comparing Model 2 (dashed lines) with model 3 (solid line) and the cluster giants ( $\times$ 's). The giant branches of the models coincide over a large range of luminosity. The point of model 3 at  $\log T_{\text{eff}} = 3.94$  and  $\log L/L_{\odot} = 1.83$  has an age of  $6.50 \times 10^8$  years, and subsequent points are separated by  $2 \times 10^8$  years.

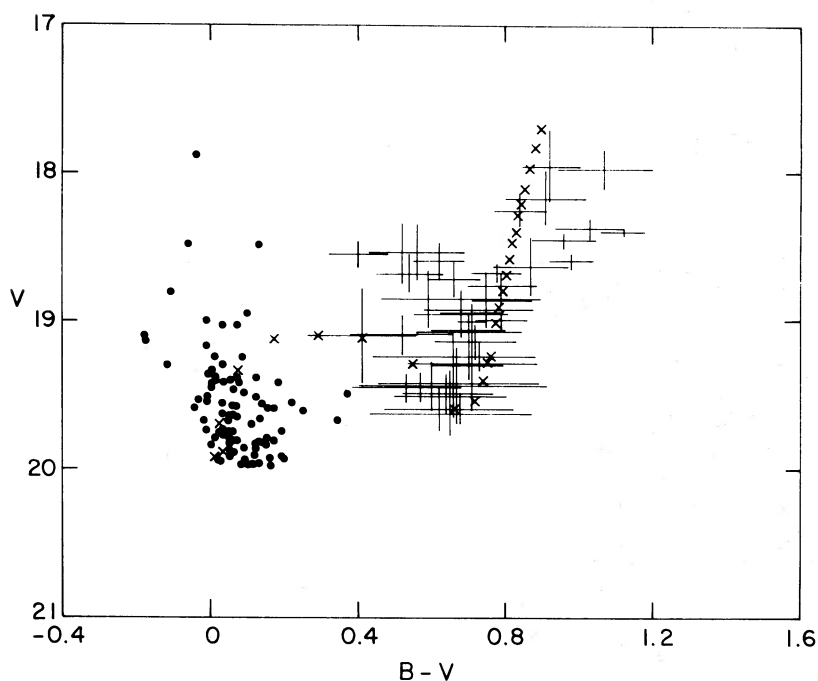


FIG. 10.—Comparison of NGC 1868 with model 3, with one standard deviation error bars plotted for the giants to display the reliability of the comparison.

to be a blue loop that is not reached by the model calculations as discussed above, and (2) the brighter red giants are too red compared to the model, i.e., the slope of the observed red giant branch is not matched well by model 3. A further reduction in  $Z$  might, in fact, change the slope of the theoretical red giant branch. Model calculations by Becker, Iben, and Tuggle (1977), and by Wagner (1978) show that if the metallicity is low enough, core helium ignition can take place before the model begins to ascend the red giant branch, thus reducing the slope of the theoretical red giant branch. From the calculations of Alcock and Paczyński (1978) we estimate that for masses less than  $2 M_{\odot}$ , the metallicity must be  $Z < 0.001$ . Hence, a further reduction in mass and in  $Z$  relative to model 3 could conceivably produce a theoretical distribution of giants that will give a better match to the observed giants in NGC 1868.

In summary, NGC 1868 is an intermediate-age ( $7 \times 10^8$  year) “blue globular” cluster of low metals abundance. Its existence shows that the present nearly

solar heavy-element abundance in the LMC must be either relatively recent or localized. It would be of great interest to examine a number of clusters in different parts of the LMC and with ages in the range  $10^8$ – $10^9$  years to piece together a complete picture of the history of heavy-element production in that galaxy. High-precision photometry and further extensive theoretical computations will be needed. Furthermore, the existence and state of evolution of superluminous stars, lying above the giant branch in NGC 1868 and in several other LMC clusters, is not understood; additional observational and theoretical research on these stars would be of great interest.

We would like to thank David Muchmore for helping with the evolutionary computations, Caty Pilachowski for several enlightening discussions, and Daris Healy and David Azose for their usual excellent work on the figures and finder charts. This research was partially funded by NSF grant AST 76-17598A01, which we also gratefully acknowledge.

#### APPENDIX

We present here details of the three theoretical tracks generated with the modified Paczyński code. Details of this code are given elsewhere (Flower 1976). Each model computed about 600 evolutionary points. Model 1 was followed to the beginning of the asymptotic branch; model 2 was followed to the near tip of the giant branch. We have chosen about 40 representative points, which are given for each model in Table 6. The points marked with asterisks are separated by equal time intervals, starting with the first point so marked

in each model. In model 1, the first point marked has an age of  $4.02 \times 10^8$  years from the zero-age main sequence, and the marked points are separated by  $10^7$  years. In model 2, the first marked point has an age of  $4.97 \times 10^8$  years, and the points with asterisks are again separated by  $10^7$  years. In model 3 the first age is  $6.50 \times 10^8$  years, and the interval is  $2 \times 10^8$  years. Figure 11 shows model 1, while models 2 and 3 are shown in Figure 9.

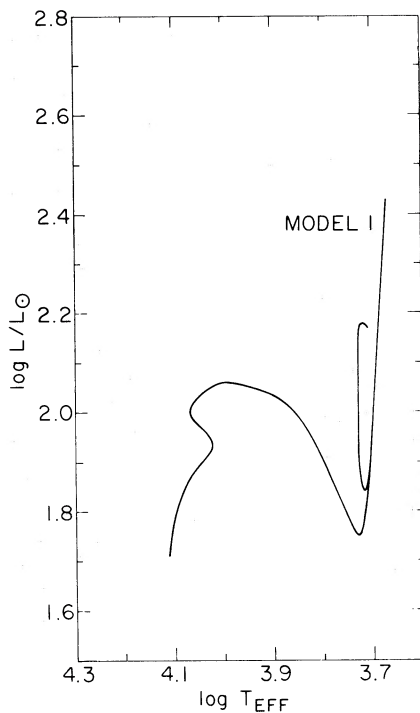


FIG. 11.—Theoretical evolutionary track for model 1

TABLE 6

log $T_{\text{eff}}$	log $L/L_{\odot}$	log $T_{\text{eff}}$	log $L/L_{\odot}$	log $T_{\text{eff}}$	log $L/L_{\odot}$
Model 1		Model 2		Model 3	
4.112	1.71	4.113	1.57	4.098	1.40
4.059	1.88	4.069	1.77	4.087	1.52
4.024	1.93	4.037	1.83	4.064	1.60
4.068	2.00	4.078	1.89	4.037	1.65
3.996	2.06	3.991	1.97	4.075	1.72
3.848*	1.99	3.898*	1.95	4.060	1.76
3.791	1.92	3.825	1.91	4.002	1.83
3.726	1.75	3.755	1.80	3.943*	1.83
3.712	1.82	3.738	1.74	3.895*	1.82
3.691	2.13	3.711	2.02	3.851*	1.80
3.682	2.26	3.703	2.15	3.776*	1.76
3.676*	2.35	3.699	2.23	3.742*	1.66
3.672	2.41	3.695	2.29	3.729*	1.70
3.670	2.43	3.693*	2.33	3.724*	1.76
3.687	2.18	3.690	2.37	3.721*	1.81
3.689	2.15	3.690	2.39	3.718*	1.87
3.694	2.08	3.691	2.37	3.715*	1.92
3.700*	1.99	3.710	2.04	3.713*	1.97
3.707	1.89	3.712	1.99	3.710*	2.01
3.715*	1.84	3.716*	1.93	3.708*	2.06
3.728*	1.89	3.726*	1.83	3.706*	2.10
3.728*	1.91	3.739*	1.87	3.704*	2.15
3.729*	1.94	3.752*	1.94	3.702*	2.19
3.729*	1.96	3.751*	1.97	3.700*	2.23
3.729*	1.99	3.753*	1.99	3.698*	2.27
3.729*	2.02	3.752*	2.02	3.696*	2.31
3.729*	2.04	3.753*	2.05	3.693*	2.37
3.729*	2.08	3.753*	2.07	3.689*	2.43
3.729*	2.10	3.754*	2.10	3.686*	2.49
3.278*	2.13	3.755*	2.13	3.685*	2.52
3.727*	2.15	3.755*	2.16	3.683*	2.56
3.724*	2.17	3.753*	2.19	3.678*	2.65
3.719*	2.18	3.751*	2.21	3.673*	2.74
3.709	2.17	3.747*	2.23		
		3.729*	2.23		
		3.699*	2.33		
		3.675	2.71		

## REFERENCES

- Alcock, G., and Paczyński, B. 1978, *Ap. J.*, **223**, 244.  
 Arp, H. C., and Thackeray, A. D. 1967, *Ap. J.*, **149**, 73.  
 Baird, S., Flower, P., Hodge, P., and Szkody, P. 1974, *A.J.*, **79**, 1365.  
 Becker, S. A., Iben, I., Jr., and Tuggle, R. S. 1977, *Ap. J.*, **218**, 633.  
 Bell, R. A., and Gustafsson, B. 1978, *Astr. Ap. Suppl.*, **34**, 229.  
 Ciardullo, R. B., and Demarque, P. 1977, *Trans. Astr. Obs. Yale Univ.*, vol. 33.  
 de Vaucouleurs, G. 1978, *Ap. J.*, **223**, 351 (and following papers).  
 Flower, P. J. 1976, Ph.D. thesis, University of Washington.  
 Flower, P. J., and Hodge, P. W. 1975, *Ap. J.*, **196**, 369.  
 Freeman, K. C., and Gascoigne, S. C. B. 1977, *Proc. Astr. Soc. Australia*, **3**, 136.  
 Gascoigne, S. C. B. 1966, *M.N.R.A.S.*, **134**, 59.  
 Gascoigne, S. C. B., Norris, J., Bessell, M. S., Hyland, A. R., and Visvanathan, N. 1976, *Ap. J. (Letters)*, **209**, L25.  
 Gustafsson, B., Bell, R. A., and Hejlesen, P. M. 1977, *Ap. J. (Letters)*, **216**, L7.  
 Harris, G. L. H., and Dupree, R. G. 1976, *Ap. J.*, **209**, 402.  
 Hartwick, F. D. A., Hesser, J. E., and McClure, R. D. 1972, *Ap. J.*, **174**, 557.  
 Hodge, P. W. 1961a, *Ap. J.*, **133**, 413.  
 ———. 1961b, *Ap. J. Suppl.*, **6**, 235.  
 ———. 1963, *Ap. J.*, **137**, 1033.  
 Hodge, P. W., and Wright, F. 1969, *Ap. J. Suppl.*, **17**, 467.  
 Iben, I., and Tuggle, R. 1975, *Ap. J.*, **197**, 39.  
 Meyer-Hofmesiter, E. 1969, *Astr. Ap.*, **2**, 143.  
 Pickering, E. C. 1891, *Ann. Harvard College Obs.*, **26**, xiv.  
 Racine, R. 1969, *A.J.*, **74**, 1073.  
 Robertson, J. W. 1974, *Ap. J.*, **180**, 425.  
 Tift, W. G., and Connolly, L. P. 1973, *M.N.R.A.S.*, **163**, 93.  
 Wagner, R. L. 1978, *Astr. Ap.*, **62**, 9.  
 Walker, M. F. 1979, *M.N.R.A.S.*, **186**, 767.  
 Woolley, R. 1960, *M.N.R.A.S.*, **120**, 214.

PHILLIP J. FLOWER: Department of Physics and Astronomy, Clemson University, Clemson, SC 29631

DOUG GEISLER, PAUL HODGE, and EDWARD OLSZEWSKI: Department of Astronomy, University of Washington, Seattle, WA 98195